Soft Matter

PAPER

Check for updates

Cite this: *Soft Matter*, 2018, **14**, 2870

White zein colloidal particles: synthesis and characterization of their optical properties on the single particle level and in concentrated suspensions†

F. Y. de Boer, [a] R. N. U. Kok, [a] A. Imhof *[a] and K. P. Velikov [abc]

Received 8th December 2017,
Accepted 17th March 2018

DOI: 10.1039/c7sm02415k

rsc.li/soft-matter-journal

Growing interest in using natural, biodegradable ingredients for food products leads to an increase in research for alternative sources of functional ingredients. One alternative is zein, a water-insoluble protein from corn. Here, a method to investigate the optical properties of white zein colloidal particles is presented in both diluted and concentrated suspensions. The particles are synthesized, after purification of zein, by anti-solvent precipitation. Mean particle diameters ranged from 35 to 135 nm based on dynamic light scattering. The value of these particles as white colorant is examined by measuring their optical properties. Dilute suspensions are prepared to measure the extinction cross section of individual particles and this was combined with Mie theory to determine a refractive index (RI) of 1.49 ± 0.01 for zein particles dispersed in water. This value is used to further model the optical properties of concentrated suspensions. To obtain full opacity of the suspension, comparable to 0.1–0.2 wt% suspensions of TiO_2, concentrations of 2 to 3.3 wt% of zein particles are sufficient. The optimal size for maximal scattering efficiency is explored by modeling dilute and concentrated samples with RI's matching those of zein and TiO_2 particles in water. The transport mean free path of light was determined experimentally and theoretically and the agreement between the transport mean free path calculated from the model and the measured value is better than 30%. Such particles have the potential to be an all-natural edible alternative for TiO_2 as white colorant in wet food products.

Introduction

Designed colloidal particles from various synthetic materials have found numerous applications in many industries ranging from food[1] to pharmaceuticals[2] and from ink[3] to displays.[4] This is because colloidal particles offer many possibilities to control product appearance through the manipulation of particle size, composition, and shape.[5] This originates from the ability of colloids to interact with light. Control of scattering and absorption of light by individual particles determines the appearance of consumer products. When organized in more complex structures, such as concentrated suspension or even colloidal crystals, multiple scattering and interference of scattered light modify the appearance further. Product appearance is an important factor that determines the perceived quality of the product by a consumer. Color and other appearance attributes create the first impression encountered by consumers; it has been shown to be of primary importance in the initial judgment of food, ultimately influencing the acceptance or rejection of the food product.[6–8] Color of particles in a suspension, is determined by a combination of the sensitivity of the human eye, illumination effects, structure, shape and size of the particles, and actual color of the product. Next to the well-known synthetic pathways to design colloidal particles, the use of sustainable and environmentally friendly materials offers additional possibilities for the control of structure, stability and compatibility of colloidal particles with various consumer products.

Currently, titanium dioxide (TiO_2) is the best known and most widely used white food colorant. Scattering of the low absorbing and high RI of the TiO_2 particles causes the whiteness that is observed. TiO_2 is authorized for use in the European Union as E171 and is used in foods such as dairy products and candy. Despite this, concerns have been raised recently regarding the toxicity of nanosized TiO_2 following oral exposure.[9] However, no conclusive results are available on this topic and research towards the safety of TiO_2 as a food additive is

[a] *Soft Condensed Matter, Debye Institute for Nanomaterials Science, Utrecht University, Princetonplein 1, Utrecht, 3584 CC, The Netherlands. E-mail: a.imhof@uu.nl*
[b] *Unilever R&D Vlaardingen, Olivier van Noortlaan 120, 3133 AT Vlaardingen, The Netherlands*
[c] *Institute of Physics, University of Amsterdam, Science Park 904, 1098 XH Amsterdam, The Netherlands*

† Electronic supplementary information (ESI) available. See DOI: 10.1039/c7sm02415k

This journal is © The Royal Society of Chemistry 2018

still ongoing.[9–11] According to the current regulations TiO_2 is considered safe as food additive, but all natural fully edible alternatives are highly desirable.

A natural and bio-based class of materials to use and synthesize colloidal particles from is the class of prolamins (*e.g.* zein, hordein and kafirin). These proteins are extracted as by-product from the seeds of cereal grains. They have many advantageous properties which make these proteins suitable for possible applications in the food industry: they are edible, renewable, and biodegradable. Moreover, they are soluble in a mixture of food safe solvents, such as 85/15 (w/w) ethanol/water; and they have good water barrier properties, both in particulate form and as films.[1,12–16] Because of these advantageous properties towards food applications, many researchers have investigated the use of zein, a prolamin from corn, for these applications.[17,18]

Zein is a group of highly hydrophobic proteins and consists of three major types of zein: α-zein (MW 19–24 kDa), β-zein (MW 17–18 kDa) and γ-zein (27 kDa).[19] The mechanism of formation of zein colloidal particles is well established.[20] Zein particles are often synthesized *via* the anti-solvent technique, resulting in particles with a positive surface charge.[21,22] This positive surface charge often leads to unwanted precipitation of these particles when added to aqueous food products. This can be overcome by using steric stabilizers such as sodium caseinate,[21,23,24] a combination of Pluronic F68 and lecithin[25] or fish gelatin and sodium alginate.[26]

Recently, zein has been proposed as a fat analogue for fats that are present in mayonnaise.[27] It has also been shown that zein is able to encapsulate colorants for use in certain food applications,[28,29] or that it can be used for triggered release purposes.[30] However, it was not investigated whether zein can be used as a white colorant in food applications to serve as an all-natural and edible replacement for the inorganic TiO_2. Therefore, in this paper we will investigate the possible use of zein as an alternative white colorant for wet food products such as mayonnaise, dressings and beverages.

In this paper, the whiteness of zein particles in suspension is investigated, as a proof of principle, in which no more components were added to the suspension than necessary. Similar to TiO_2, the whiteness of the zein particles is due to low absorption and strong scattering by the particles. However, the RI is lower in this case, which means that the concentration needs to be increased for a similar opacity. For the synthesis of white particles, zein is first purified to remove colored impurities.[31,32] Then white zein nanoparticles are synthesized in a range of sizes using anti-solvent precipitation.[22,33–35] The value of these nanoparticles as white colorant is quantified by measuring their scattering properties. The extinction cross section is measured on the single particle level; from this the refractive index (RI) of the zein particles in water can be determined by fitting Mie theory to the data. Transparent and opaque suspensions of zein nanoparticles are obtained by varying the concentration of particles in solution. The obtained suspensions are used to compare the zein particles to aqueous suspensions of TiO_2, which has a much higher RI. The optimal particle size necessary for obtaining a maximal scattering efficiency is explored by modeling. This was done both for dilute and concentrated samples, using RI's that match those of white zein (1.49) and TiO_2 particles (2.5688) in water (1.333). Finally, and most importantly, the whiteness resulting from multiple scattering of light is quantified for more concentrated suspensions, and expressed in terms of the transport mean free path. The obtained results are then compared to multiple scattering theory. For future research is interesting to investigate the interaction between food components and zein particles after addition to real food systems.

Methods

Materials

Ethanol (100% pure) was obtained from Interchema. Hydrochloric acid (HCl) was purchased from Sigma Aldrich. Food grade TiO_2 QS (geometric particle size 376 nm and geometric particle size distribution 1.34) was obtained from ChemoPharma. Zein was purchased from Flo Chemical Corporation (Zein F4000C-FG, lot no. F40006011C6) and water was purified using a Millipore Direct-Q purification system.

Methods

Purification of zein powder. Colored impurities present in the zein were removed by washing zein powder in ethanol. Zein (10 g) was stirred in ethanol (1.5 L) overnight, after which the suspension was left to sediment by gravity. The supernatant was discarded and the sediment was collected. This was repeated two more times. The sediment was used to create a 10 wt% stock solution by dissolving it in 85 wt% aqueous ethanol. In order to completely dissolve the sediment, the solution was heated to 45 °C while stirring, after which the solution was cooled to room temperature on air. Small aggregates were removed by filtration using a 0.45 μm filter (PVDF, Millipore). The resulting solution is further referred to as stock solution.

Preparation of white zein nanoparticles. 10 mL of stock solution was quickly added to a beaker with water (120 mL) while stirring at 280 rpm with a stir bar. A two-day dialysis of the resulting suspension against water adjusted to a pH of 4 with HCl was used to completely remove the ethanol; during this dialysis, the medium was replaced 4 times. Dialysis tubing membranes were purchased at Sigma-Aldrich, and had a molecular weight cut-off of 14 000 Da, as this will retain the 3 major types of zein: α-zein (MW 19–24 kDa), β-zein (MW 17–18 kDa) and γ-zein (27 kDa).[19] The resulting colloidal suspension was centrifuged for 30 minutes at 222 rcf to remove possible large aggregates. Finally, the samples were stored in the fridge at 5 °C. Samples were stored for a maximum of two weeks before measurement. The dry weight of the zein stock solutions and colloidal suspensions were determined by weighing an amount of the solution or suspension, letting the liquid evaporate at 120 °C for 2 hours, and then measuring the dry weight.

Particle shape, size and charge. Particle sizes and charges were measured by dynamic light scattering (DLS) and electrophoresis,

using a Zetasizer Nano ZS series, Malvern Instruments. In DLS a CONTIN analysis was used to obtain the size distributions. Prior to the DLS and zeta potential measurements, the samples were diluted, with water adjusted to pH 4, to a suitable concentration, where the samples appear almost completely transparent to the eye, to prevent multiple scattering. Scanning electron microscopy (SEM), Nova Nanolab, FEI, was used for determining the particle shape. To minimize changes in particle size and shape, samples were freeze-dried overnight using a lyophilizer (Virtis). The dry powder, which was loosely attached to the lyophilizing bottle, was collected and stored in a desiccator until SEM analysis. Prior to SEM analysis a platinum layer of about 4 nm was sputtered onto these samples to prevent charging.

Determination of optical properties. UV-Vis spectroscopy (HP 8953A spectrophotometer) was used for several purposes: verification of the purification process; determination of the extinction cross sections of the particles; and for comparative experiments between the opacity of zein particles and TiO_2 particles. Quartz cuvettes of 1 and 10 mm were used.

The purification process was verified by measuring absorption spectra of purified and unpurified solutions of 10 wt% zein and spectra of supernatants of three washing steps. For this purpose, also coatings were made from one unpurified and one purified solution of zein of 10 wt% by applying these solutions, with a brush, onto Leneta cards which were dried in air. These cards were illuminated by the standard daylight illuminant, D65; and images were taken using a DigiEye (VeriVide). The extinction cross sections of the zein particles were obtained by measuring absorption spectra of dilute suspensions of zein particles. Prior to the measurements, samples were diluted with water pH 4, adjusted with HCl, to suitably low concentrations, where the samples appear almost completely transparent to the eye, to prevent multiple scattering. Final concentrations were, depending on the particle size, between 0.06 wt% (for small particles) and 0.01 wt% (for large particles). The final concentration of each sample was measured by determination of the dry weight of the particles in the suspension. For a comparative study between the opacity of zein and TiO_2 particles, zein particles were concentrated using a centrifugal concentrator (Vivaspin 20, pore size 100 000 Da, Sartorius) at a pressure of 3 bar without centrifugation, and then measured at various concentrations. These results were compared to food grade TiO_2 particles in aqueous suspensions of 0.01, 0.1 and 0.2 wt%.

Color determination. The color of strongly scattering samples was determined using total reflectance spectroscopy, which was measured on a home-built set-up. Experiments were carried out with a spectrophotometer (HR4000, Ocean Optics) equipped with a 15 cm diameter integrating sphere (barium sulfate coated, Labsphere) with a sample opening of 12 mm, an opening for the detector port of 3 mm and an opening for the light beam of 6 mm. The total reflectance of concentrated samples was measured using a cylindrical 10 mm quartz cuvette, in the visible wavelength range. As a light source, a Tungsten Halogen light source (HL-2000-FHSA-LL, Ocean Optics) was used and at the detection port a multimode fiber was used to couple the light into a spectrometer (HR4000, Ocean Optics). For a schematic overview of the setup see Fig. S1 (ESI†).

Optical properties of concentrated suspensions. The transport mean free path (l^*) was experimentally determined *via* total transmittance spectroscopy. Measurements were carried out using a home-built setup with a spectrophotometer equipped with an integrating sphere; this setup used the same components as the total reflectance setup, but in a slightly different configuration, see Fig. S2 (ESI†). The entrance opening of the sphere was 18 mm in diameter and the detector port opening 3 mm. Concentrated samples were measured in cylindrical quartz cuvettes (series 120-QS, Hellma Analytics), with path lengths 1, 2, and 5 mm at wavelengths ranging from 400 to 800 nm.

Results and discussion

Purification of zein

In order to synthesize white particles, zein powder was purified to remove impurities that result in a yellow color, which is attributed to xanthophylls and β-carotene.[31,32] This purification was carried out by washing zein in 100% ethanol, in which the zein does not dissolve,[12] but the colored impurities do.[36] The number of washing steps necessary was determined by collecting the supernatants of three consecutive washing steps and measuring their absorption spectra (Fig. 1a). These results indicate that one washing step is already sufficient to remove most removable impurities from the zein; this is the number of steps used for particle synthesis. To verify that the impurities due to colorants were indeed removed, the absorption spectra of solutions of unpurified and purified (three washing steps) zein solutions were compared by UV-Vis spectroscopy (Fig. 1b). After purification, a lower absorption is observed in the wavelength range 300 to 500 nm than for the unpurified zein, which again indicates that most of the removable impurities were successfully removed. To visualize the effect in a more direct way, coatings were made from one unpurified and one purified solution of zein of 10 wt%, (Fig. 1c and d). These coatings confirm that there were indeed colored impurities in the raw zein as this coating has a yellow appearance. After washing with ethanol, the color is removed to a large extent.

Particle shape, size and charge

The purified zein stock solution was used to prepare colloidal suspensions using anti-solvent precipitation (Fig. 2a). The particle size of the resulting colloids was tuned by varying the concentration of zein in the stock solution. In SEM it can be observed that the particles are spherical and very polydisperse, see Fig. 2b, which is according to expectations.[37] Data on the particle size obtained through SEM are presented in Fig. S3 (ESI†). The samples were prepared with different mean particle sizes, ranging from 35 to 135 nm in diameter (number distribution from DLS), see Fig. 2c. Particle size distributions are presented in Fig. S4 (ESI†). It is observed that the polydispersity, defined as the standard deviation of the distribution, increased with increasing particle size, which is according to expectations.[20,25] The high

 This journal is © The Royal Society of Chemistry 2018

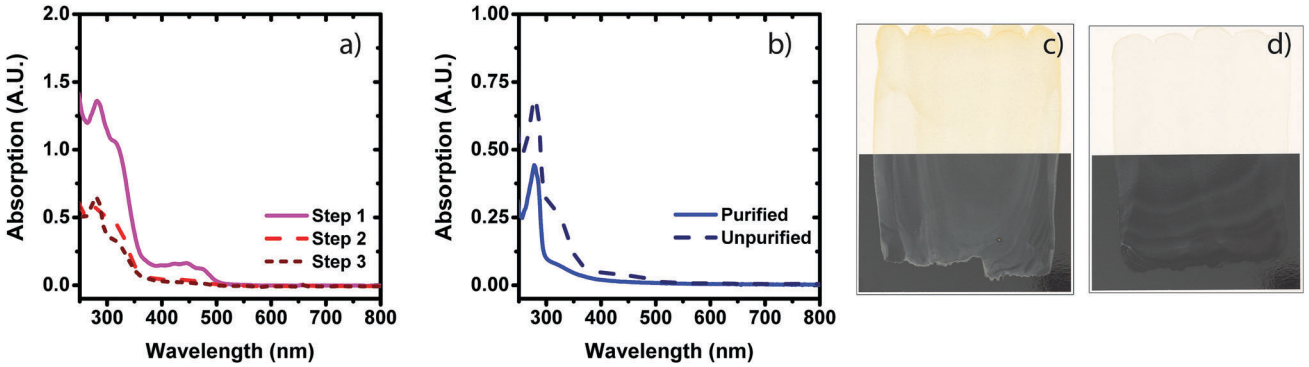

Fig. 1 UV-Vis absorption spectra showing the effect of purification of zein, by removal of colored impurities by washing zein with ethanol: (a) supernatants after one, two and three washing steps. (b) Purified (after three washing steps) and unpurified solutions of zein. Optical photographs of coatings made from 10 wt% solutions of (c) purified zein and (d) unpurified zein on half-white-half-black Leneta cards. Samples were illuminated by the standard daylight illuminant D65; images were taken using the DigiEye.

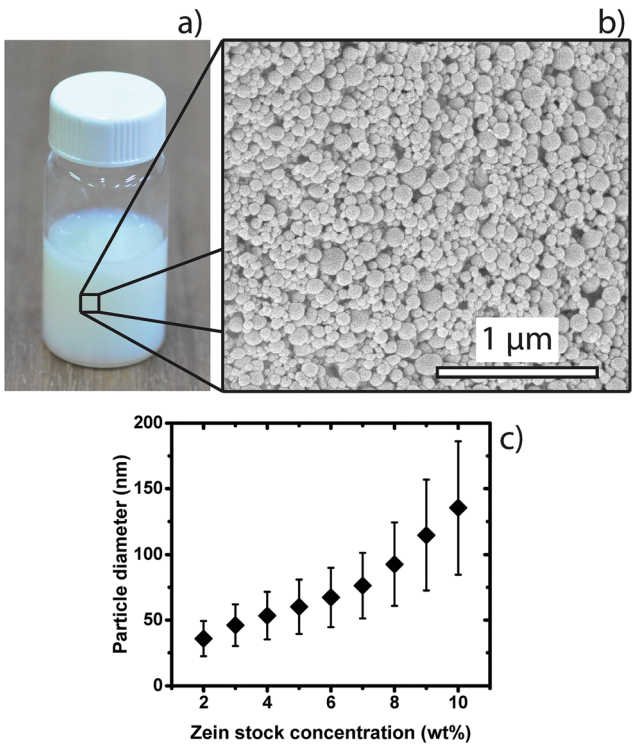

Fig. 2 (a) A suspension of white zein particles synthesized from an 8 wt% stock solution. (b) An SEM image of these particles after freeze drying, particles were spherical and had an average diameter of 91 ± 29 nm (counted from SEM images). A whole range of particle sizes could be synthesized when varying the concentration of zein in the stock solution, mean average sizes (c) were measured in DLS. The vertical bars show the standard deviation of the size distribution from DLS.

polydispersity of the samples is a consequence of the synthesis method. It is possible to synthesize larger particles according to this method using higher zein concentrations in the stock solution. However, then polydispersity will increase, and the particle yield and reproducibility will be low due to severe aggregation. The zeta-potential of the particles varied between 40 and 50 mV for all samples with no specific relation to the particle size. These results are according to expectations.[21,24] These values are sufficiently high to stabilize the particles without the need for additional stabilizers.

Determination of color and opacity

The visual appearance of the colloidal suspensions was determined by total reflectance spectroscopy. From the total reflectance results, the tristimulus values and chromaticity coordinates were calculated[38] and visualized in a CIE color diagram; see Fig. 3a, where the white point is included as a reference point for optimal whiteness in the CIE color diagram. The zein colloidal particles have a color very close to the white point, which means that the sample is observed as white, making a suitable white colorant.

The hiding power of the white zein particles was determined by their transmission and were compared to food grade TiO_2 particles which functions as a benchmark. The white zein colloids scatter short wavelengths more strongly than long wavelengths, so transmission is higher towards the red wavelength area, as seen in Fig. 3b. To obtain an opaque suspension of zein particles, the higher transmission in the red can be reduced by increasing the concentration of the zein particles in the suspension. Another option would be to increase the particle diameter, since larger particles scatter more strongly. However, processing conditions used here only allow sizes up to about 135 nm. TiO_2 is known and used for its good scattering properties, which are a result of its high refractive index (2.5688 for anatase[39]). Therefore, food grade TiO_2 particles in aqueous suspensions of 0.01, 0.1 and 0.2 wt% were used as a benchmark. To obtain high opacity suspensions, a relatively low concentration of 0.2 wt% TiO_2 particles is more than sufficient (Fig. 3c). Since zein particles have a lower refractive index, at similar concentrations, more transparent suspensions are obtained. It is important to note that the zein particles are considerably smaller than the TiO_2 particles, which further limits the achievable opacity of the zein samples. However, when higher concentrations of zein particles are used, a similar opacity can be achieved as for the lower concentrations of TiO_2 particles. An increase in concentration of zein particles of two to seventeen times (2 to 3 wt% zein particles) is needed compared to TiO_2, depending on the wavelength, to achieve a similar transparency.

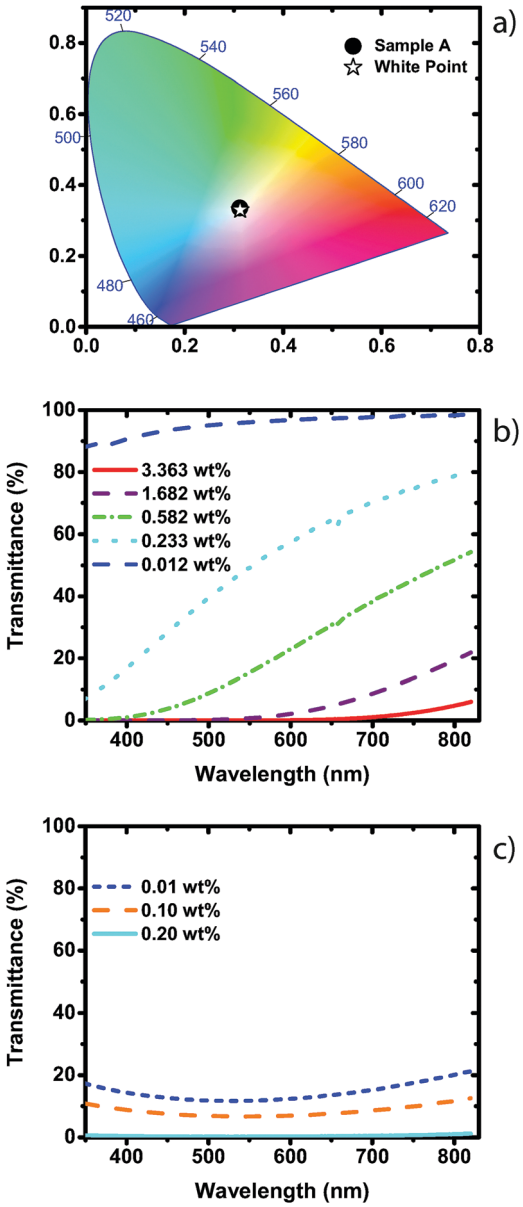

Fig. 3 (a) CIE diagram of synthesized zein particles of sample A. Sample A has a particle diameter of 115 ± 41 nm and a concentration of 1.9 wt% and was compared to the theoretical white point. Transmission spectra at various concentrations of (b) white zein particles (diameter is 122 ± 49 nm) and (c) food grade TiO_2 particles (diameter is 376 nm).

Modeling and experiments on dilute suspensions

To obtain a colloidal suspension with a white appearance it is important to use particles with optimal scattering efficiency. This can be modeled using Mie theory, which describes the scattering of light by spherical particles.[40] In a transmission measurement the extinction is measured, which is the sum of scattering and absorption. For modeling of the white zein particles, it is assumed that there is no absorption, so that the extinction efficiency is equal to the scattering efficiency. However, since the particles may still absorb slightly, the term extinction will be used.

The quantity to consider is the extinction cross section per unit volume of scattering material. We will see shortly that this has a maximum for a particular, optimal, radius. To evaluate the theory, MiePlot software created by Philip Laven[41] was used. To use this model for zein particles, the RI of the particles in water should be known in advance. The RI of dry zein fibers is reported[42,43] to be 1.54 or 1.55. In this study there are no dry fibers, but particles dispersed in water. This makes it very likely that there is some water trapped in the colloidal particles which will lower the RI of the particles compared to dry zein. Common methods to determine the RI, such as refractive index matching measurements, were not an option, since it impossible to predict the swelling behavior of the zein particles in other solvents. Moreover, zein is soluble in a large number solvents.[44] Therefore, experiments and theory are combined, by measuring the extinction on the single particle level and comparing this to the model in which the RI is a variable.

Lambert Beer's law was used to obtain the extinction efficiency. The transmitted intensity I is related to the extinction cross section C_{ext} per particle as:

$$I = I_0 \mathrm{e}^{-\rho C_{\mathrm{ext}} L} \tag{1}$$

Here, I_0 is the incident intensity and L the path length of the cuvette. The number density of particles ρ is obtained from the weight concentration of the suspension $c_z = 4\pi r^3 \rho D_z/3$, assuming spherical particles with radius r and mass density D_z (1.1 g cm^{-3}). Introducing the extinction $A = -\log(I/I_0)$, eqn (1) can be rewritten as:

$$\frac{Q_{\mathrm{ext}}}{r} = A \ln(10) \frac{4D_z}{3c_z L} \tag{2}$$

Here, $Q_{\mathrm{ext}} = C_{\mathrm{ext}}/\pi r^2$ is the extinction efficiency. This equation shows that the extinction is maximized by maximizing Q_{ext}/r. This quantity is essentially the scattering cross section per unit volume of scattering material: when a given volume of material is used to make spherical particles the extinction will be maximal when the particles are given the radius that maximizes Q_{ext}/r. Eqn (2) was used to obtain Q_{ext}/r for synthesized zein particles. In Fig. 4 the squares show these data plotted *versus* the average radius for several wavelengths ranging from 450 to 700 nm. As seen, Q_{ext}/r increases with r as all particle sizes are well below the optimal radius. Also, Q_{ext}/r increases as the wavelength decreases. For a correct comparison of these measurements with theory, the latter should take into account the polydispersity of the corresponding experimental system. Since each particle scatters independently and in proportion to its extinction efficiency, eqn (1) should be replaced by:

$$I = I_0 \mathrm{e}^{-\rho \sum_i f_i C_{\mathrm{ext},i} L} \tag{3}$$

where f_i is the fraction of particles of size r_i. Since now $c_z = \rho \sum_i 4\pi r_i^3 f_i D_z/3$, this can be written as:

$$\left\langle \frac{Q_{\mathrm{ext}}}{r} \right\rangle \equiv \frac{\sum f_i r_i^3 \frac{Q_{\mathrm{ext},i}}{r_i}}{\sum f_i r_i^3} = A \ln(10) \frac{4D_z}{3c_z L} \tag{4}$$

This journal is © The Royal Society of Chemistry 2018

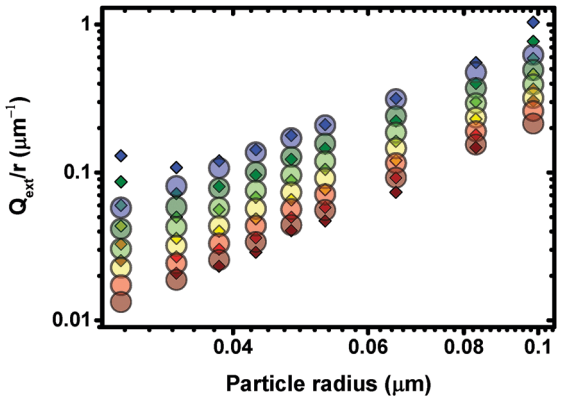

Fig. 4 $\langle Q_{ext}/r \rangle$ *versus* average particle radius measured on dilute samples (small squares) and calculated from Mie theory (large circles). Input for the theory is: a particle refractive index of 1.49, a particle density of 1.1 g cm^{-3}, and the measured particle volume distribution from DLS for each sample. Data are shown for six wavelengths, shown in colors from blue to red: 450, 500, 550, 600, 650, 700 nm.

Thus, $\langle Q_{ext,i}/r_i \rangle$ should be averaged over the particle size distribution, using as weights the factors $f_i r_i^3$, which describe the distribution of particle volumes, rather than radii. This distribution is readily obtained from dynamic light scattering. The theoretical data (circles in Fig. 4) were calculated in MiePlot according to eqn (4) using the volume distributions from DLS experiments on the corresponding samples (Fig. S5, ESI†). To achieve this, a RI of the medium water at 20 °C was used, and for zein particles a RI of 1.49. This resulted in good agreement with experimental results. When a higher RI was used the theoretical points shifted up, and when a lower RI was used the theoretical points shifted down. Fig. S6 and S7 (ESI†) show that the RI's of 1.48 or 1.50 result in a noticeably poorer agreement, from these results it can be concluded that the RI of these particles is 1.49 ± 0.01.

Now it is possible to determine the optimal size for maximal extinction efficiency completely by the model, using 1.49 as input for the RI. Results, calculated using MiePlot, are shown in Fig. 5a at a few wavelengths spanning the visible spectrum. This indicates that particles with an RI of 1.49 in water should have a diameter between 700 and 1000 nm to reach their optimal extinction efficiency, which is much larger than particles that were synthesized in this study. For comparison, Fig. 5b includes the same model for TiO_2 particles (RI = 2.5688)[45] in water.

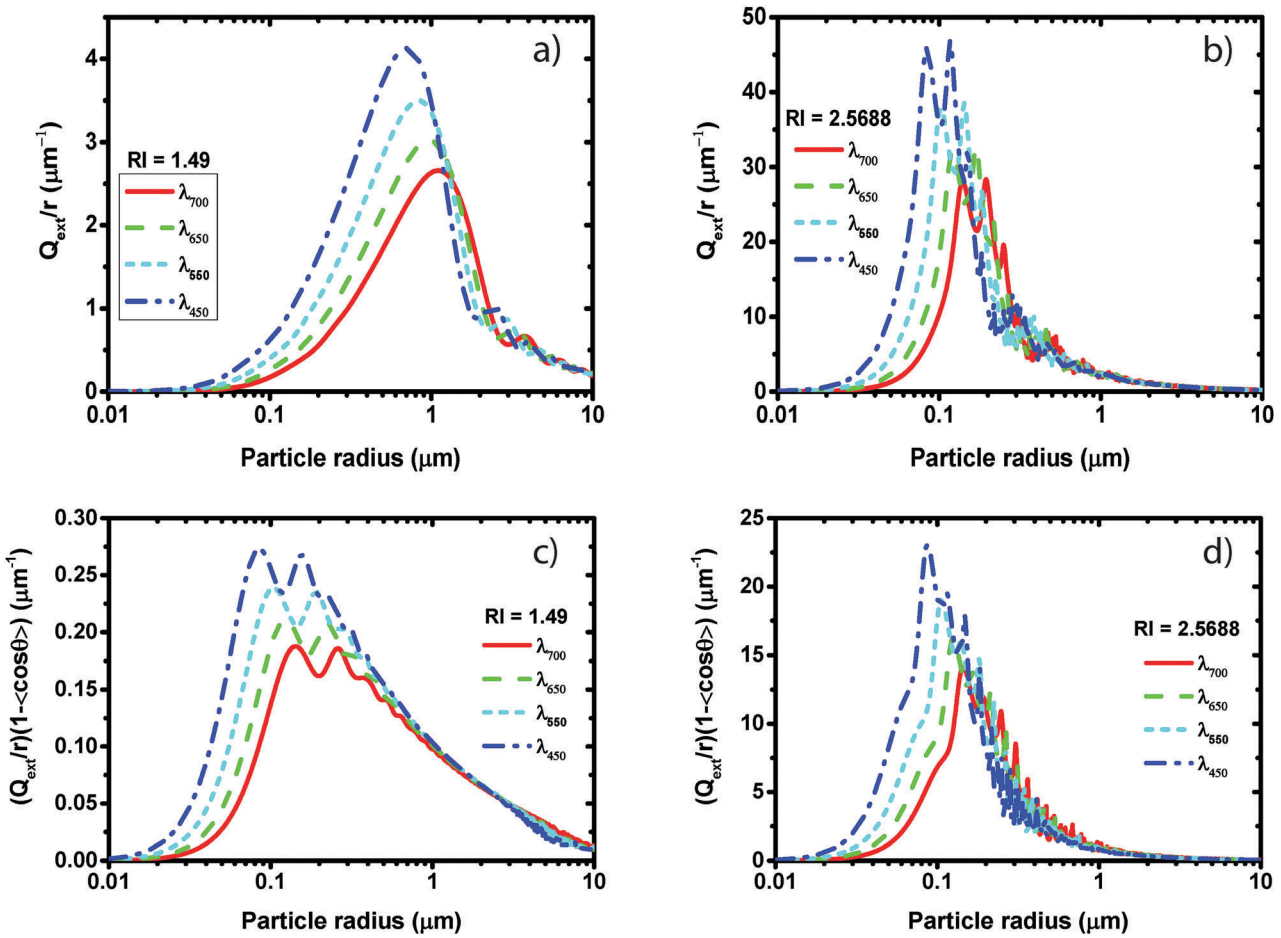

Fig. 5 Single particle scattering model: Q_{ext}/r *versus* the particle radius for monodisperse particles with a refractive index (RI) of (a) 1.49 (zein) and (b) 2.5688 (TiO_2), with water as medium. Scattering model for concentrated suspensions: $(Q_{ext}/r)(1 - \langle\cos\theta\rangle)$ *versus* the particle radius for monodisperse particles of which the particles have a refractive index of (c) 1.49 (zein) and (d) 2.5688 (TiO_2). Calculations were done at four wavelengths in the visible spectrum.

Here the optimal particle size is much smaller, which has its origin at the higher RI ratio of the particles and the medium. Finally, comparison of the vertical scales of Fig. 5a and b shows that TiO_2 scatters just about 10 times more strongly than zein on a per volume basis. Note that these Mie scattering calculations describe single scattering only. Multiple scattering will change the picture drastically, as will be shown next.

Modeling and experiments on concentrated suspensions

In systems where the interest is in whiteness of the suspension, the sample is concentrated. This means that light is scattered not once but multiple times before leaving the sample. The quantity $\rho C_{ext} = 1/l$ is called the inverse of the scattering mean free path (when absorption is absent). In this equation l is a measure for the average distance that a light ray travels in the sample before it scatters. In the dilute samples discussed so far light will scatter at most once, and so $l \gg L$. In concentrated samples, the scattering strength is quantified by the transport mean free path, l^*, which describes the distance over which the direction of propagation of light is randomized. l^* is closely related to l, but in addition includes the average of the cosine of the scattering angle, or anisotropy factor, which can also be calculated from Mie theory:[46]

$$\frac{1}{l^*} = \frac{1 - \langle \cos\theta \rangle}{l} \tag{5}$$

Using eqn (5), $\rho = 3c_z/(4D_z\pi r^3)$ and $Q_{ext} = C_{ext}/\pi r^2$, eqn (1) can be rewritten analogously to eqn (2):

$$\frac{Q_{ext}}{r}(1 - \langle \cos\theta \rangle) = \frac{1}{l^*}\frac{4D_z}{3c_z} \tag{6}$$

Thus, the left-hand side shows the quantity to maximize, in order to minimize the total transmittance (and maximize diffuse reflectance) of a multiply scattering sample at a fixed weight concentration. Note that here the assumption is made that the scattering particles are uncorrelated, which is the case for the relatively low concentrations (<3 wt%) used in this work. Again, MiePlot can be used for the calculation of Q_{ext} and $\langle \cos\theta \rangle$. Fig. 5c and d show results of calculations from MiePlot for spheres of RI 1.49 and 2.5688 at several visible wavelengths in water. The optimal particle diameter now ranges from 100 to 250 nm in the case of zein particles, which is much smaller than for single scattering, and just within reach of the here presented synthesis. For TiO_2 particles, on the other hand, such a shift is not observed and the optimum of the scattering efficiency stays at a similar position. However, the absolute values are much higher. Again, when comparing the vertical scales of Fig. 5c and d it is observed that TiO_2 scatters about 10 times more strongly that zein on a per volume basis. This indicates that by using a high enough concentration it is possible to achieve similar scattering properties for zein particles as for TiO_2 particles, as is also indicated in Fig. 3b and c.

A common way to experimentally determine the transport mean free path is from the relation[47] between the total transmittance T, and the path length of the cell, L (eqn (7)),

$$T = (1 - R_s)\frac{1 + z_e}{\frac{L}{l^*} + 2z_e}, \quad \text{with } z_e = \frac{2}{3}\left(\frac{1 + \bar{R}}{1 - \bar{R}}\right) \tag{7}$$

which shows that total diffuse transmittance is low at small l^*. In this situation, most of the incident light is diffusely reflected (neglecting absorption).

Here, $\bar{R}$ is the polarization and angle-averaged internal diffuse reflectivity of the sample, R_s is the specular reflectivity of the incident light beam from the front face of the sample, and z_e is the extrapolation length ratio that describes the boundary conditions of the diffuse intensity at the interface of the sample. R_s and $\bar{R}$ can be calculated *via* Fresnel's reflection coefficients as described by Vera and Durian[48] from the RI's of the sample medium, container wall, and external medium (*i.e.* 1.330, 1.458, and 1.000 respectively), which leads to $R_s = 0.0367$ and $z_e = 1.7365$. Finally, l^* is obtained from the slope of the linear fit of the $1/T$ *vs.* L plot. To compare experimental data to theory eqn (6) has to be averaged over the particle size distribution. For a multicomponent system l^* is given by:[49]

$$\frac{1}{l^*} = \rho \sum_i f_i C_{ext,i}\left(1 - \langle \cos\theta \rangle_i\right) \tag{8}$$

In a similar way as before eqn (8) can be rewritten in a more useful form:

$$\left\langle \frac{Q_{ext}}{r}(1 - \langle \cos\theta \rangle) \right\rangle \equiv \frac{\sum_i f_i r_i^3 \frac{Q_{ext,i}}{r_i}\left(1 - \langle \cos\theta \rangle_i\right)}{\sum_i f_i r_i^3} = \frac{1}{l^*}\frac{4D_z}{3c_z} \tag{9}$$

The particle volume distribution $f_i r_i^3$ is again taken from DLS results of the corresponding samples. Results are shown in Fig. 6. Deviations between experimental results and theoretical calculations, as prescribed by eqn (9), are seen to be on average about 30%. This is still the case when different particle sizes or different volume fractions are used (sample A, B and C in Fig. (6)). All samples in Fig. (6) show an increase in the transport mean free path when the wavelength increases. This is a trend which is consistent with that observed in literature for ensembles of highly polydisperse non-absorbing nanoparticle scatterers.[47,50,51] In these works a similar accuracy is obtained between experiment and theory. It can be observed that the values of the experimental results are always below the theoretical data, which indicates that the particles scatter more than expected. An explanation might be that part of the transmitted light was captured by the integrating sphere, but escaped at the edges of the sample holders. Despite this, the qualitative agreement between theory and experiment is good. Fig. 6 shows that the models of samples B and C cross at a wavelength between 600 and 650; this is also visible for the experimental results. This indicates that experiments, synthesis, and total transmittance measurements are very sensitive, and therefore have a good agreement with theory.

 This journal is © The Royal Society of Chemistry 2018

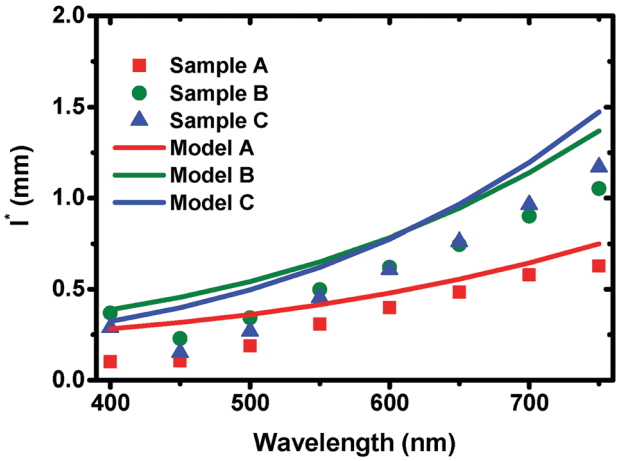

Fig. 6 The transport mean free path, *l**, found experimentally by total transmittance spectroscopy (points) and calculated from theory (lines) of three zein particle suspensions with different mean particle sizes. Sample A had a particle diameter of 115 ± 41 nm and 1.9 wt%, sample B a diameter of 93 ± 32 nm and 1.6 wt%, and sample C a diameter of 76 ± 41 nm and 2.3 wt%.

Conclusions

In this study white zein colloidal particles were successfully synthesized *via* anti-solvent precipitation after removal of colored impurities present in zein. Average particle diameters of the synthesized nanoparticles were varied between 35 and 135 nm. The value of the zein nanoparticles as white colorant was examined by measuring their optical properties. Dilute suspensions were prepared to measure the extinction cross section on the single particle level. Opaque suspensions of zein particles were obtained by increasing the concentration of zein particles in suspension. Compared to TiO_2 particles in suspension a higher concentration of zein particles was necessary to obtain a similar opacity. In this work, a method was devised to determine the RI of the white zein particles by fitting experimental results on dilute, but polydisperse, samples with Mie theory. It was found to be 1.49 ± 0.01, which was then used to model optical properties and the transport mean free path for strongly scattering suspensions. The agreement between the transport mean free path calculated from the model and the measured value is better than about 30%.

These results show that it is possible to model the scattering behavior of suspensions of zein particles. This makes it possible to synthesize zein nanoparticles with specifically designed optical properties, which can be tuned towards a specific application. The combination of the food safe ingredients of this system and the simple anti-solvent precipitation technique together with dialysis, show great potential for usage of these particles as natural white colorant and clouding agent for application in wet food products and beverages.

Conflicts of interest

There are no conflicts to declare.

Acknowledgements

This research is supported by the Dutch Technology Foundation STW (grant 13567), which is part of the Netherlands Organization for Scientific Research (NWO) and partly funded by the Ministry of Economic Affairs. We would like to thank Jantina Fokkema for proofreading the manuscript.

References

1 I. J. Joye and D. J. McClements, *Curr. Opin. Colloid Interface Sci.*, 2014, **19**, 417–427.
2 R. Paliwal and S. Palakurthi, *J. Controlled Release*, 2014, **189**, 108–122.
3 M. Elgammal, R. Schneider and M. Gradzielski, *Dyes Pigm.*, 2016, **133**, 467–478.
4 Y. Wang, E. L. Runnerstrom and D. J. Milliron, *Annu. Rev. Chem. Biomol. Eng.*, 2016, **7**, 283–304.
5 K. P. Velikov and E. Pelan, *Soft Matter*, 2008, **4**, 1964–1980.
6 N. Imram, *Nutr. Food Sci.*, 1999, **99**, 224–230.
7 F. J. Francis, *Food Qual. Prefer.*, 1995, **6**, 149–155.
8 S. R. Gifford and F. M. Clydesdale, *J. Food Prot.*, 1986, **49**, 977–982.
9 R. J. B. Peters, G. Van Bemmel, Z. Herrera-Rivera, H. P. F. G. Helsper, H. J. P. Marvin, S. Weigel, P. C. Tromp, A. G. Oomen, A. G. Rietveld and H. Bouwmeester, *J. Agric. Food Chem.*, 2014, **62**, 6285–6293.
10 Y. Yang, K. Doudrick, X. Bi, K. Hristovski, P. Herckes, P. Westerhoff and R. Kaegi, *Environ. Sci. Technol.*, 2014, **48**, 6391–6400.
11 A. Weir, P. Westerhoff, L. Fabricius, K. Hristovski and N. Von Goetz, *Environ. Sci. Technol.*, 2012, **46**, 2242–2250.
12 R. Shukla and M. Cheryan, *Ind. Crops Prod.*, 2001, **13**, 171–192.
13 M. A. Del Nobile, A. Conte, A. L. Incoronato and O. Panza, *J. Food Eng.*, 2008, **89**, 57–63.
14 Y. Luo, T. T. Y. Wang, Z. Teng, P. Chen, J. Sun and Q. Wang, *Food Chem.*, 2013, **139**, 224–230.
15 M. P. M. Garcia, M. C. Gómez-Guillén, M. E. López-Caballero and G. V. Barbosa-Cánovas, *Edible Films and Coatings: Fundamentals and Applications*, CRC Press, 2016.
16 J. Xiao, Y. Li, J. Li, A. P. Gonzalez, Q. Xia and Q. Huang, *J. Agric. Food Chem.*, 2015, **63**, 216–224.
17 I. J. Joye and D. J. McClements, *Trends Food Sci. Technol.*, 2013, **34**, 109–123.
18 A. R. Patel and K. P. Velikov, *Curr. Opin. Colloid Interface Sci.*, 2014, **19**, 450–458.
19 S.-Z. Wang and A. Esen, *Plant Physiol.*, 1986, **81**, 70–74.
20 Q. Zhong and M. Jin, *Food Hydrocolloids*, 2009, **23**, 2380–2387.
21 A. R. Patel, E. C. M. Bouwens and K. P. Velikov, *J. Agric. Food Chem.*, 2010, **58**, 12497–12503.
22 N. Chatsisvili, A. P. Philipse, B. Loppinet and R. H. Tromp, *Food Hydrocolloids*, 2017, **65**, 17–23.
23 Y. Feng and Y. Lee, *Food Hydrocolloids*, 2016, **56**, 292–302.

24 Y. Zhang, Y. Niu, Y. Luo, M. Ge, T. Yang, L. Yu and Q. Wang, *Food Chem.*, 2014, **142**, 269–275.
25 S. Podaralla and O. Perumal, *AAPS PharmSciTech*, 2012, **13**, 919–927.
26 K. Yao, W. Chen, F. Song, D. J. McClements and K. Hu, *Food Hydrocolloids*, 2017, **79**, 262–272.
27 J. Gu, Z. Xin, X. Meng, S. Sun, Q. Qiao and H. Deng, *J. Food Eng.*, 2016, **182**, 1–8.
28 X. W. Chen, S. Y. Fu, J. J. Hou, J. Guo, J. M. Wang and X. Q. Yang, *Food Chem.*, 2016, **211**, 836–844.
29 A. R. Patel, P. C. M. Heussen, E. Dorst, J. Hazekamp and K. P. Velikov, *Food Chem.*, 2013, **141**, 1466–1471.
30 M. Nieuwland, N. E. Papen-Bottenhuis, W. C. Drost, T. M. Slaghek and B. S. J. F. Erich, *Ind. Crops Prod.*, 2016, **83**, 353–358.
31 D. J. Sessa and K. K. Woods, *J. Am. Oil Chem. Soc.*, 2011, **88**, 1037–1043.
32 D. J. Sessa, F. J. Eller, D. E. Palmquist and J. W. Lawton, *Ind. Crops Prod.*, 2003, **18**, 55–65.
33 Y. Luo and Q. Wang, *J. Appl. Polym. Sci.*, 2014, **131**, 40696.
34 G. Davidov-Pardo, I. J. Joye and D. J. Mcclements, *Advances in Protein Chemistry and Structural Biology*, 2015, vol. 98, pp. 293–325.
35 J. W. J. de Folter, M. W. M. van Ruijven and K. P. Velikov, *Soft Matter*, 2012, **8**, 6807.
36 D. B. Rodriguez-Amaya, *A guide to carotenoid analysis in foods*, ILSI Press, Washington, D. C., 2001.
37 T. Zou, Z. Li, S. S. Percival, S. Bonard and L. Gu, *Food Hydrocolloids*, 2012, **27**, 293–300.
38 W. S. Stiles and G. Wyszecki, *J. Opt. Soc. Am.*, 1962, **52**, 313.
39 U. Diebold, *Surf. Sci. Rep.*, 2003, **48**, 53–229.
40 C. F. Bohren and D. M. Huffman, *Absorption and Scattering of Light by Small Particles*, 1983, pp. 82–129.
41 P. Laven, *MiePlot software*, http://www.philiplaven.com/mieplot.htm.
42 T. A. Trezza and J. M. Krochta, *J. Appl. Polym. Sci.*, 2001, **79**, 2221–2229.
43 W. J. Roff and J. R. Scott, *Fibres, films, plastics and rubbers: a handbook of common polymers*, Butterworth-Heinemann, London, 1971, pp. 197–204.
44 J. W. Lawton, *Cereal Chem.*, 2002, **79**, 1–18.
45 O. Ola and M. M. Maroto-Valer, *J. Photochem. Photobiol., C*, 2015, **24**, 16–42.
46 L. F. Rojas, R. Vavrin, C. Urban, J. Kohlbrecher, A. Stradner, F. Scheffold and P. Schurtenberger, *Faraday Discuss.*, 2003, **123**, 385–400.
47 W. L. Vos, T. W. Tukker, A. P. Mosk, A. Lagendijk and W. L. IJzerman, *Appl. Opt.*, 2013, **52**, 2602–2609.
48 M. U. Vera and D. J. Durian, *Phys. Rev. E: Stat. Phys., Plasmas, Fluids, Relat. Interdiscip. Top.*, 1996, **53**, 3215–3224.
49 P. D. Kaplan, A. D. Dinsmore, A. G. Yodh and D. J. Pine, *Phys. Rev. E: Stat. Phys., Plasmas, Fluids, Relat. Interdiscip. Top.*, 1994, **50**, 4827–4836.
50 J. Gómez Rivas, R. Sprik, C. M. Soukoulis, K. Busch and A. Lagendijk, *Europhys. Lett.*, 1999, **48**, 22–28.
51 V. Y. F. Leung, A. Lagendijk, T. W. Tukker, A. P. Mosk, W. L. IJzerman and W. L. Vos, *Opt. Express*, 2014, **22**, 8190–8204.

This journal is © The Royal Society of Chemistry 2018